

# Supplemental Material for Precision Measurement of Time-Reversal Symmetry Violation with Laser-Cooled Polyatomic Molecules

Ivan Kozyryev<sup>1,\*</sup> and Nicholas R. Hutzler<sup>2,1,†</sup>

<sup>1</sup>*Department of Physics, Harvard University, Cambridge, MA 02138, USA*

<sup>2</sup>*Division of Physics, Mathematics, and Astronomy,  
California Institute of Technology, Pasadena, CA 91125, USA*

(Dated: August 5, 2017)

## Molecular structure and Stark/Zeeman shifts

We shall examine the structure and Stark/Zeeman shifts of a triatomic molecular degenerate bending mode  $\nu$  with vibrational angular momentum  $\ell$  and energy  $\omega$ . Consider the case of a heavy atom at the end of the molecule with a light functional group,  $\ell = 1$ ,  $S = I = 1/2$ , with the nuclear spin not on the heavy atom, such as YbOH. The quantum numbers and couplings are  $F = I + J$  and  $J = N + S$ .  $J$  includes the degenerate bending mode angular momentum  $\ell$ , therefore  $N$  is a coupling of molecule rotation and  $\ell$  and can take the values  $N = |\ell|, |\ell| + 1, |\ell| + 2, \dots$ . We shall consider the case  $N = |\ell| = 1$ , and therefore often leave  $S, I$ , and  $N$  out of kets. We shall only consider external fields small enough that we can neglect mixing with the  $N = 2$  state.

### Zero-field

The most important interactions for us are spin-rotation, Fermi contact hyperfine, and  $\ell$ -doubling. The energy level diagram in zero external fields is shown schematically in figure 1.

*Spin-rotation:* In a diatomic  $^2\Sigma$  molecule, the spin-rotation interaction  $\gamma S \cdot N$  splits each  $N$  level into 2  $J$ -levels with  $J = N \pm 1/2$ . The physical origin is the electron spin interacting with the magnetic field of the orbiting nucleus, so it might seem odd that in the “non-rotating”  $N = |\ell| = 1$  state we get a similar interaction. Since  $\ell$  involves the rotation of a nucleus about the symmetry axis, this creates a magnetic field that interacts with the electron spin. The magnitude of this effect is empirically similar to the usual spin-rotation effect, since the  $\gamma$  constant in the  $\nu = 0$  and  $\nu = 1$  states are similar [1]. For YbOH,  $\gamma \approx 30$  MHz [2]. One can also make a simple, semi-classical argument that the magnetic field created by the rotating nucleus in both cases is similar.

Brown and Carrington [3] equation (9.89) gives the formula for the corresponding diatomic case, which therefore excludes  $\ell$ . In [1], they find that the alkaline earth hydroxide spin-rotational structure is well-described by this Hund’s case (b) Hamiltonian, so we use the diatomic

formula with the addition that  $\ell$  is not changed:

$$\begin{aligned} \langle N\ell S J I F M | H_{SR} | N\ell S J I F M \rangle = \\ \gamma \delta_{\ell\ell'} (-1)^{N+J+S} \begin{Bmatrix} S & N & J \\ N & S & 1 \end{Bmatrix} \\ \times [S(S+1)(2S+1)N(N+1)(2N+1)]^{1/2}. \quad (1) \end{aligned}$$

This interaction is diagonal in our basis, as expected.

*Hyperfine:* The hyperfine interaction consists of a Fermi contact interaction  $\beta_\eta S \cdot I$ . There is also a spin-spin interaction between  $S$  and  $I$  characterized by the constant  $c$ , but the matrix elements in this state suppress it to be much smaller than the Fermi contact, and we shall ignore it. The matrix elements for Fermi contact can be found in Hirota [4] equation (2.3.80):

$$\begin{aligned} \langle N'\ell' S' J' I' F' M' | H_{HF} | N\ell S J I F M \rangle = \\ b_\eta \delta_{MM'} \delta_{FF'} \delta_{NN'} \delta_{\ell\ell'} (-1)^{N+S+J'} (-1)^{J+I+F+1} \\ \times [S(S+1)(2S+1)I(I+1)(2I+1)]^{1/2} \\ \times [(2J'+1)(2J+1)]^{1/2} \begin{Bmatrix} I & J' & F \\ J & I & 1 \end{Bmatrix} \begin{Bmatrix} S & J' & N \\ J & S & 1 \end{Bmatrix} \quad (2) \end{aligned}$$

The constant  $b_\eta$  is also written as  $b_\eta = b - c/3$ . For proton hyperfine from an OH group, such as in YbOH,  $b \approx c \approx b_\eta \approx 2$  MHz [5].

*$\ell$ -doubling:* Since  $\ell$  breaks parity symmetry, the zero-field (parity,  $P$ ) eigenstates are

$$|\pm, J, F, M\rangle = \frac{|+\ell, J, F, M\rangle \pm |-\ell, J, F, M\rangle}{\sqrt{2}}. \quad (3)$$

Because  $\ell$  is the projection of  $J$  onto the symmetry axis, it is very analogous to  $\Omega$  for the case of a diatomic, and  $K$  for the case of a symmetric top. In fact, for a degenerate bending mode  $\nu$ , the state  $\nu = \ell = 1$  correlates to  $K = 1, \nu = 0$  [6]. Coriolis interactions lift the degeneracy between the opposite-parity states  $\pm$  and result in  $\ell$ -type doubling. Each state  $|\pm, J, F, M\rangle$  acquires an energy shift of  $\pm \frac{1}{2} q N(N+1) = \pm q$ . The magnitude of this effect is generally the same order as the vibration-rotation interaction constant  $\alpha$ , defined as  $B_\nu = B_e - \alpha(\nu+1)$ , and is generally of order  $\sim B_e^2/\omega$  [7]. For YbOH, we can use the value of  $q \approx -10$  MHz from another heavy hydroxide BaOH, since the rotational constant and vibrational energy are similar [1].

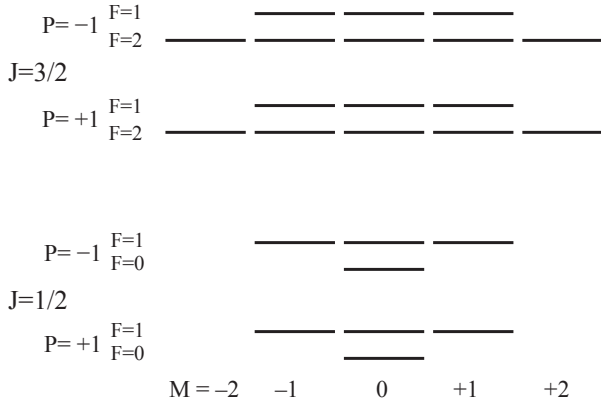


FIG. 1. Structure of a  $^2\Sigma$  electronic,  $N = |\ell| = 1$ ,  $S = I = 1/2$  state in zero field. The scale (both relative and overall) and ordering of levels may not be accurate for every molecule, but are representative of YbOH.

### Stark effect

We shall only consider  $M \geq 0$ , keeping in mind that the Stark shifts are even in  $M$  by parity symmetry. The matrix elements of the Stark Hamiltonian  $H_S$  of an electric field  $\mathcal{E}$  in the lab  $z$ -direction are given by Hirota [4] equation (2.5.35):

$$\begin{aligned} \langle N'\ell'SJ'IF'M' | H_S | N\ell SJIFM \rangle = & \\ \mathcal{E} d(-1)^{F'-M'} \begin{pmatrix} F' & 1 & F \\ -M' & 0 & M \end{pmatrix} & \\ \times (-1)^{J'+I+F+1} [(2F'+1)(2F+1)]^{1/2} \begin{Bmatrix} J' & F' & I \\ F & J & 1 \end{Bmatrix} & \\ \times (-1)^{N'+S+J+1} [(2J'+1)(2J+1)]^{1/2} \begin{Bmatrix} N' & J' & S \\ J & N & 1 \end{Bmatrix} & \\ \times (-1)^{N'-\ell'} \begin{pmatrix} N' & 1 & N \\ -\ell' & 0 & \ell \end{pmatrix}, & \quad (4) \end{aligned}$$

where we have taken  $p = q = 0$ , written  $T_{p=0}^1(E) = \mathcal{E}$  and  $T_{q=0}^1(d) = d$ , and set  $K \rightarrow \ell$ . Note that the first and last lines of this formula look just like a Hund's case (a) or (c), with the middle two lines coming from the couplings  $F = I + J$  and  $J = N + S$ , respectively.

Consider the stretched states with  $M = \pm 2$ . These are very simple to understand since there are only four states in this manifold ( $M = \pm 2$ ,  $P = \pm 1$ ,  $J = 3/2$ ,  $F = 2$ ), all matrix elements conserve  $M$ , and the Stark matrix elements are

$$\begin{aligned} \langle P', J = 3/2, F = 2, M' | H_S | P, J = 3/2, F = 2, M \rangle & \\ = \begin{cases} -1/2 & P' \neq P, M' = M \\ 0 & \text{otherwise} \end{cases} & \quad (5) \end{aligned}$$

This means that the fully-polarized eigenstates are states of good  $\pm M, \pm \ell$ , i.e. fully mixed parity. If we examine

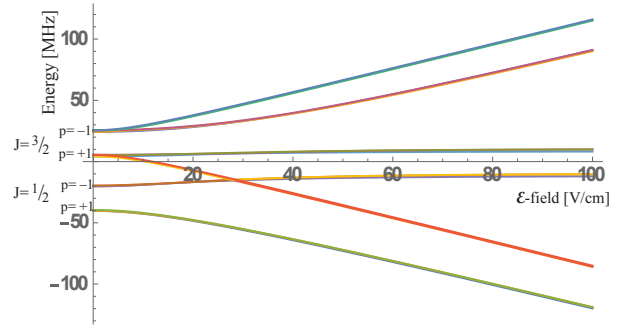


FIG. 2. Stark shifts with  $\gamma = 30$  MHz,  $q = -10$  MHz,  $b = 2$  MHz, and  $d = 4$  D, representative of YbOH. There are several avoided and unavoided crossings. The states are labeled on the left side by their zero-field quantum numbers.

the eigenstates individually, we see that the sign of the Stark shift is  $\propto -M\ell$ , which is reminiscent of the Stark shift in a  $\Omega > 0$  diatomic state of  $\propto -M\Omega$ .

Table I shows the composition of the eigenstates in a 250 V/cm field in terms of the zero-field eigenstates. There is an almost-symmetry between the top and bottom half of the table; flipping the parity in the table would yield nearly the same table (up to signs), except for a few states that have different relative admixtures of  $F$  values in  $\pm P$  (for example, the states in columns 2 and 3). These states also have the additional interesting feature that they have  $M = 0$  and therefore no linear Zeeman shifts but do have linear Stark shifts.

### Zeeman Shifts

Now let's apply a magnetic field in the  $z$ -direction. We shall again only consider  $M \geq 0$ , keeping in mind that the (relevant) linear Zeeman shifts are odd in  $M$ . We will work under the conditions where the Zeeman shift is smaller than any other energy splitting, so we can treat the effect perturbatively. We will also ignore any "small" effects, such as nuclear spin, rotation, and quadratic Zeeman shifts, considering only linear magnetic interactions from the electron spin with the applied field. The matrix elements are given by Hirota (2.5.16):

$$\begin{aligned} \langle N'\ell'SJ'IF'M' | H_Z | N\ell SJIFM \rangle = & \\ \delta_{NN'} \delta_{\ell\ell'} (-1)^{F'-M} [(2F'+1)(2F+1)]^{1/2} \begin{pmatrix} F' & 1 & F \\ -M' & 0 & M \end{pmatrix} & \\ \times (-1)^{F'+I+F+1} [(2J'+1)(2J+1)]^{1/2} \begin{Bmatrix} J' & F' & I \\ F & J & 1 \end{Bmatrix} & \\ \times (-1)^{N'+S+J'+1} [S(S+1)(2S+1)]^{1/2} \begin{Bmatrix} S & J' & N \\ J & S & 1 \end{Bmatrix} & \quad (6) \end{aligned}$$

We can find the Zeeman shifts in the polarized limit by taking the eigenstates in some  $\mathcal{E}$ -field and finding

the expectation of the Zeeman operator. The results are shown in table I.

$J$	$F$	$M$	$P$																
1/2	0	0	-1	0.	0.	35.3	0.	0.	1.3	0.	0.	0.	-33.3	0.	0.	0.	-30.	0.	0.
1/2	1	0	-1	0.	35.3	0.	0.	0.	0.	1.6	0.	-33.	0.	0.	0.	-30.	0.	0.	0.
1/2	1	1	-1	35.3	0.	0.	0.	0.	0.	0.	1.5	0.	-33.2	-29.9	0.	0.	0.	0.	0.
3/2	1	0	-1	0.	12.6	0.	0.	0.	0.	0.	-0.1	0.	65.3	0.	0.	-22.	0.	0.	0.
3/2	1	1	-1	-3.9	0.	0.	35.3	0.	0.	0.	0.	0.	0.	-16.3	6.6	0.	0.	-37.9	0.
3/2	2	0	-1	0.	0.	12.6	0.	0.	0.	0.	0.	0.	65.3	0.	0.	0.	-22.	0.	0.
3/2	2	1	-1	8.8	0.	0.	12.7	0.	0.	0.	0.	0.	0.	48.9	-15.5	0.	0.	-14.	0.
3/2	2	2	-1	0.	0.	0.	0.	48.	0.	0.	0.	0.	0.	0.	0.	0.	0.	0.	-52.
1/2	0	0	+1	0.	38.6	0.	0.	0.	0.	-33.4	0.	0.	0.	0.	0.	28.	0.	0.	0.
1/2	1	0	+1	0.	0.	38.6	0.	0.	-33.3	0.	0.	0.	0.	0.	0.	28.	0.	0.	0.
1/2	1	1	+1	38.5	0.	0.	0.	0.	0.	0.	-33.4	0.	0.	0.	27.9	0.	0.	0.	0.
3/2	1	0	+1	0.	0.	13.4	0.	0.	0.	65.3	0.	0.	1.3	0.	0.	0.	19.9	0.	0.
3/2	1	1	+1	-4.1	0.	0.	38.3	0.	0.	0.	-16.2	0.	0.	-0.4	-6.	0.	0.	35.	0.
3/2	2	0	+1	0.	13.4	0.	0.	0.	0.	64.9	0.	1.7	0.	0.	0.	20.	0.	0.	0.
3/2	2	1	+1	9.4	0.	0.	13.7	0.	0.	0.	48.8	0.	0.	1.1	14.	0.	0.	12.9	0.
3/2	2	2	+1	0.	0.	0.	0.	52.	0.	0.	0.	0.	0.	0.	0.	0.	0.	0.	48.
$\Delta_Z$				-0.985	0.	0.	0.998	1.	0.	0.	0.986	0.	0.	0.986	-0.981	0.	0.	0.997	1.
$P_E$				-0.993	-0.993	-0.993	-0.999	-0.999	0.001	0.001	0.001	0.	0.001	0.001	0.991	0.991	0.991	0.999	0.999
$M$ :				1	0	0	1	2	0	0	1	0	0	1	1	0	0	1	2

TABLE I. Table of admixtures with a 250 V/cm electric field, assuming  $\gamma = 30$  MHz,  $b = 2$  MHz,  $q = -10$  MHz, and  $d = 4$  D. The values are fractional admixtures of amplitude (in percent), where the sign indicates the sign of the contribution before squaring. At the bottom we list the signed electric polarization  $P_E$ , the Zeeman shift in units of  $\mu_B \mathcal{B}$ , and the value of  $M$ , which is conserved for our case.

### Estimate of Franck-Condon factors for polyatomics

The FCFs for YbOH are shown in table II. Similar estimates for YbCCH, YbOCH<sub>3</sub>, and YbCH<sub>3</sub> indicate that two dominant FCFs for Yb-ligand stretching vibrations sum to  $\gtrsim 0.95$  for all of these species, making them all promising candidates for laser cooling. While including anharmonic terms in the molecular potential will improve the accuracy of the calculation, the relative magnitudes of the loss channels as well as the total sum of the dominant FCFs should not change significantly as indicated by our SrOH studies [9]. Our calculated FCFs for YbOH are comparable to those measured for the iso-electronic diatomic molecule YbF [10]. With four vibrational repumpers indicated in figure 3 of the main paper, each YbOH molecule will scatter on average  $10^4$  photons. Adding a repumping laser for (400) vibrational state will result in scattering approximately  $5 \times 10^4$  photons per molecule.

### Populating the excited vibrational state

Even though  $\Delta l_2 \neq 0$  vibronic transitions are forbidden in the Born-Oppenheimer (BO) approximation, optical excitation of the nominally forbidden  $\tilde{X}(000) \rightarrow \tilde{A}(010)$  transition has been previously observed for al-

Transition	FCF	VBR
$\tilde{X}^2\Sigma^+ - \tilde{A}^2\Pi_{1/2}$		
(000)-(000)	0.8670	0.8786
(100)-(000)	0.1173	0.1083
(200)-(000)	0.0133	0.0111
(300)-(000)	0.0013	0.0010
(400)-(000)	$1 \times 10^{-4}$	$8 \times 10^{-5}$
(020)-(000)	0.0010	0.0009
(001)-(000)	$2 \times 10^{-5}$	$1 \times 10^{-5}$

TABLE II. Estimated Franck-Condon factors (FCF) and vibrational branching ratios (VBR) for the  $\tilde{X} - \tilde{A}$  transition in <sup>174</sup>YbOH. The calculation was performed assuming the harmonic oscillator approximation of molecular vibrations using methods from Ref. [8]. Measured YbOH molecular constants from Ref. [2] were used as input. Our calculations were initially benchmarked by comparing measured and calculated FCFs for SrOH [9] and showed close agreement.

kaline earth monohydroxides. The spin-orbit (SO) vibronic Renner-Teller couplings  $H_{RT} \times H_{SO}$  mix  $\tilde{A}^2\Sigma^+$  and  $\tilde{B}^2\Pi$  states with  $v_2 = \pm 1$  and  $\Delta l_2 = -\Delta \Lambda = \pm 1$  resulting in the BO approximation breakdown [11]. Assuming comparable size of the Renner-Teller parameter  $\epsilon$ , the magnitude of the forbidden transition probability should scale as  $A_{SO}^2/\Delta E_{\Sigma-\Pi}^2$  which is approximately the same value for BaOH and YbOH. Previous experimental measurements for BaOH [12] show comparable strength

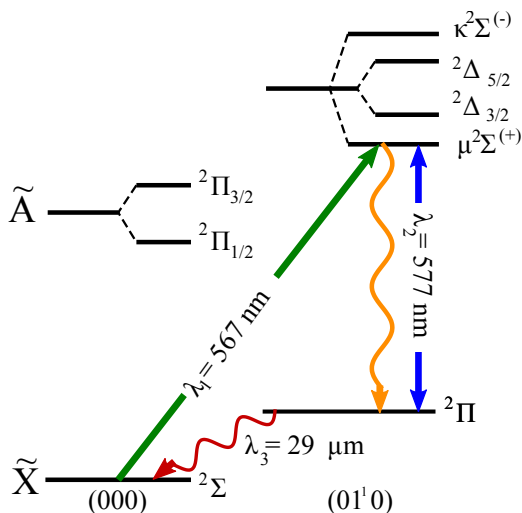


FIG. 3. Proposed optical pumping scheme for YbOH in order to populate the excited bending state (010). Vibronic species of the relevant states are indicated. Optical readout of the molecular population in (010) state can be performed via direct excitation with  $\lambda_2$ . The  $\tilde{A}$  state splits into four distinct states due to the spin-orbit and Renner-Teller interactions. The energy splittings are not to scale.

of the allowed  $(02^00) - (000)$  and forbidden  $(010) - (000)$  bands. Efficient optical pumping into the excited bending state  $\tilde{X}(010)$  via  $\tilde{X}^2\Sigma^+(000) \rightarrow \tilde{A}(010)\mu^2\Sigma^{(+)}$  off-diagonal excitation should be possible as previously experimentally seen for SrOH [11]. Figure 3 depicts the optical pumping scheme that can be used for transferring YbOH molecules from the vibrational ground state to the (010) excited bending mode where the T-violating effects will be measured. Alternatively, optical pumping can be replaced with coherent Raman transfer [13] leading to greater efficiency during the state transfer process.

### Estimate of vibrational lifetimes

To estimate the lifetime of the YbOH  $\nu_2 = 1$  excited bending mode, we use the measured excitation energy  $\sim 300 \text{ cm}^{-1}$  and estimated  $(000)-(010)$  transition dipole moment of 0.1 D [14, 15] to compute an Einstein A-coefficient of  $\sim 0.1 \text{ s}^{-1}$ , or a lifetime of  $\gtrsim 10 \text{ s}$ . Black-body radiation (BBR) can also induce vibrational decays, but we estimate that this effect at 300 K should be lower than the spontaneous decay rate by  $\sim 1/4$  and therefore will not limit the experimental coherence time. Additionally, reducing the chamber temperature to 77 K will reduce  $\Gamma_{\text{BBR}}$  by a factor of 400. Our estimations are consistent with the previous analysis of black-body limited vibrational lifetimes for diatomic molecules [16, 17].

### Laser cooling with multiple ground states

Coupling multiple ground states to a few excited states results in reduction of the effective scattering rate and, correspondingly, decreased radiative force [18]. Decoupling of the main cycling transition  $\lambda_0$  from multiple repumping lasers will lead to rapid optical cycling at multiple MHz rates. Spectroscopy of the isoelectronic molecule YbF indicates the presence of the  $\tilde{B}^2\Sigma^+$  molecular state originating from the  $4f^{14}6p\sigma$  atomic orbital of the Yb<sup>+</sup> ion [19]. Repumping the (020), (200), and (300) excited vibrational levels through the  $\tilde{B}$  state will increase the cycling rate by a factor of 2.3 leading to stronger radiative force. Moreover, promotion of the  $f$  electrons into the unfilled excited orbitals leads to additional electronic states not present in alkaline earth monohydroxides. Repumping through such levels has been considered possible for YbF [20] and should work for YbOH as well for repumping dark vibrational states which are infrequently populated (e.g. (300)).

The use of coherent stimulated optical forces instead of traditional radiative techniques for beam deceleration and cooling will significantly reduce the number of required spontaneous emissions. Particularly, the bichromatic force has been extensively investigated theoretically for complex multilevel molecules [21] and recently demonstrated experimentally for a triatomic molecule SrOH [9].

### Symmetric tops

Since the energy of symmetric top molecules is the same for clockwise and counterclockwise rotations around the top symmetry axis, the states with  $\pm K$  should have the same energy, where  $K$  is the projection of the total rotational, orbital, and vibrational angular momentum on the symmetry axis. Since the ground electronic and vibrational levels of molecules isoelectronic to YbOH like YbCH<sub>3</sub> and YbOCH<sub>3</sub> have no orbital or vibrational angular momenta,  $K$  solely represents the projection of rotational angular momentum  $R$ . The presence of any interaction that directly or indirectly couples the  $\pm K$  results in the eigenstates  $|R, +K\rangle \pm |R, -K\rangle$ , which represent doublets of opposite parity. Like  $\ell$ -doublets for linear triatomics in excited bending levels, such  $K$ -type doublets arise from a slight molecular asymmetry but the doublet splitting is typically much smaller. Previous studies have shown that for XCH<sub>3</sub> type molecules, the largest doublet splitting is for  $|K| = 1$  levels and arises from H spin-rotation and X-H spin-spin coupling resulting in kHz-wide splittings. Splittings between  $K$ -doublets for  $K \geq 2$  are significantly smaller, with about  $10^{-4} \text{ Hz}$  for  $K = 2$  [22]. Consequently, complete polarization of symmetric top molecules is possible for rotational states with  $K \neq 0$  in very small laboratory

electric fields of  $\sim 1$  mV/cm [22, 23] which is even smaller than for  $\ell$ -doublets.

The lowest rotational level of each  $K$  has energy  $\approx AK^2$ . Therefore, compared to the  $\sim 10$  THz excitation energies of the lowest bending mode levels with non-zero  $\ell$  of YbOH, the excited  $K = 1$  states with opposite parity  $K$  doublets are typically only  $\sim 160$  GHz above the absolute vibronic ground state for symmetric top YbCH<sub>3</sub> and YbOCH<sub>3</sub>. Thus, the spontaneous decay lifetimes are typically well over one minute. Since ortho and para configurations of the CH<sub>3</sub> group of XCH<sub>3</sub> and XYCH<sub>3</sub> molecules do not efficiently cool into each other in the collisions associated with supersonic expansion cooling [24], we anticipate that a large fraction of molecules in  $K = 1$  rotational levels will also be created during the buffer-gas cooling process as previously seen for some symmetric tops [25]. Alternatively, direct optical pumping into excited  $K$  levels is possible by using perpendicular optical transitions with  $\Delta K = \pm 1$  selection rule (e.g.  $\tilde{X} - \tilde{A}$  band for SrCH<sub>3</sub> and SrOCH<sub>3</sub> [24]). The cylindrical symmetry of symmetric tops enables well-defined rotational selection rules that can be used to achieve optical cycling on a quasi-closed transition with only a few laser frequencies. The specific details of achieving optical cycling in alkaline earth monoalkoxides MOR like CaOCH<sub>3</sub> have been laid out in detail in Ref. [26] and because of their electronic structure similarity with YbOR, the same approach is applicable here as well. Additionally, the dominant four Franck-Condon factors for YbOCH<sub>3</sub> sum up to  $> 0.99$ , indicating that efficient optical cycling and laser cooling could be achieved.

---

\* ivan@cua.harvard.edu

† hutzler@caltech.edu

- [1] D. A. Fletcher, M. A. Anderson, W. L. Barclay, and L. M. Ziurys, *The Journal of Chemical Physics* **102**, 4334 (1995).
- [2] T. C. Melville and J. A. Coxon, *The Journal of Chemical Physics* **115**, 6974 (2001).
- [3] J. Brown and A. Carrington, *Rotational Spectroscopy of Diatomic Molecules* (Cambridge University Press, 2003).
- [4] E. Hirota, *High-Resolution Spectroscopy of Transient Molecules*, Springer Series in Chemical Physics, Vol. 40 (Springer Berlin Heidelberg, Berlin, Heidelberg, 1985).
- [5] D. A. Fletcher, K. Y. Jung, C. T. Scurlock, and T. C. Steimle, *The Journal of Chemical Physics* **98**, 1837 (1993).
- [6] G. Herzberg, *Molecular Spectra and Molecular Structure, Volume 3: Electronic Spectra and Electronic Structure of Polyatomic Molecules* (D. Van Nostrand, 1967).
- [7] G. Herzberg, *Reviews of Modern Physics* **14**, 219 (1942).
- [8] T. Sharp and H. Rosenstock, *The Journal of Chemical Physics* **41**, 3453 (1964).
- [9] I. Kozyryev, *Laser cooling and inelastic collisions of the polyatomic radical SrOH*, Ph.D. thesis, Harvard University (2017).
- [10] X. Zhuang, A. Le, T. C. Steimle, N. E. Bulleid, I. J. Smallman, R. J. Hendricks, S. M. Skoff, J. J. Hudson, B. E. Sauer, E. a. Hinds, and M. R. Tarbutt, *Physical chemistry chemical physics : PCCP* (2011), 10.1039/c1cp21585j.
- [11] P. I. Presunka and J. A. Coxon, *The Journal of Chemical Physics* **101**, 201 (1994).
- [12] S. Kinsey-Nielsen, C. Brazier, and P. Bernath, *The Journal of chemical physics* **84**, 698 (1986).
- [13] C. Panda, B. O’Leary, A. West, J. Baron, P. Hess, C. Hoffman, E. Kirilov, C. Overstreet, E. West, D. DeMille, *et al.*, *Physical Review A* **93**, 052110 (2016).
- [14] M. Okumura, L. I. Yeh, D. Normand, J. J. H. van den Biesen, S. W. Bustamente, Y. T. Lee, T. J. Lee, N. C. Handy, and H. F. Schaefer, *J. Chem. Phys.* **86**, 3807 (1987).
- [15] J. Senekowitsch, S. Carter, H.-J. Werner, and P. Rosmus, *Chemical Physics Letters* **140**, 375 (1987).
- [16] N. Vanhaecke and O. Dulieu, *Molecular Physics* **105**, 1723 (2007).
- [17] S. Y. Buhmann, M. Tarbutt, S. Scheel, and E. Hinds, *Physical Review A* **78**, 052901 (2008).
- [18] M. R. Tarbutt, B. E. Sauer, J. J. Hudson, and E. A. Hinds, *New Journal of Physics* **15**, 053034 (2013).
- [19] R. F. Barrow and A. Chojnicki, *Journal of the Chemical Society, Faraday Transactions 2: Molecular and Chemical Physics* **71**, 728 (1975).
- [20] I. Smallman, F. Wang, T. Steimle, M. Tarbutt, and E. Hinds, *Journal of Molecular Spectroscopy* **300**, 3 (2014).
- [21] L. Aldridge, S. Galica, and E. Eyler, *Physical Review A* **93**, 013419 (2016).
- [22] W. Klemperer, K. Lehmann, J. Watson, and S. Wofsy, *The Journal of Physical Chemistry* **97**, 2413 (1993).
- [23] R. Butcher, C. Chardonnet, and C. J. Bordé, *Physical Review Letters* **70**, 2698 (1993).
- [24] M. Dick, P. Sheridan, J.-G. Wang, and P. Bernath, *The Journal of Chemical Physics* **124**, 174309 (2006).
- [25] X. Wu, T. Gantner, M. Zeppenfeld, S. Chervenkov, and G. Rempe, *ChemPhysChem* **17**, 3631 (2016).
- [26] I. Kozyryev, L. Baum, K. Matsuda, and J. M. Doyle, *ChemPhysChem* **17**, 3641 (2016).